

PROCEEDINGS OF SPIE

[SPIDigitalLibrary.org/conference-proceedings-of-spie](https://spiedigitallibrary.org/conference-proceedings-of-spie)

Synthetic-aperture direct-detection coherent imaging

James R. Fienup

James R. Fienup, "Synthetic-aperture direct-detection coherent imaging,"
Proc. SPIE 10410, Unconventional and Indirect Imaging, Image
Reconstruction, and Wavefront Sensing 2017, 104100B (6 September 2017);
doi: 10.1117/12.2276949

SPIE.

Event: SPIE Optical Engineering + Applications, 2017, San Diego, California,
United States

Synthetic-aperture Direct-detection Coherent Imaging

James R. Fienup

University of Rochester, Institute of Optics, Rochester, NY 14627

ABSTRACT

This paper describes an approach to coherent aperture synthesis and fine-resolution image reconstruction employing phase retrieval from intensity measurements. A Gerchberg-Saxton algorithm is used on a pair of intensity measurements to obtain the fields for each telescope at each position of the telescopes without a reference beam. These are combined into a larger synthetic aperture, and a cross-correlation is used to sense and correct for piston, tip and tilt phases of each of the sub-apertures with respect one another, giving a much higher resolution than from a single aperture. Results of simulations, including the effects of speckle, are shown, and practical considerations are evaluated.

Keywords: synthetic aperture, imaging, phase retrieval, phase-error correction, image reconstruction, heterodyne

1. INTRODUCTION

To achieve fine resolution imagery at a given long stand-off distance and in a given wavelength band, one needs a collection system (telescopes) having a large enough effective aperture. An alternative to building and deploying larger single apertures (which become increasing bulky, heavy and costly), one can perform aperture synthesis, either passively (using reflected sunlight) as in Michelson stellar interferometry or actively as in coherent laser illumination with phase-sensitive detection. Michelson interferometry requires two or more simultaneous apertures having substantial motion of one aperture relative to another and for a variety of reasons is poorly suited to downward looking at the earth. One could use laser SAR in which temporal or chirped frequency sensing provides range information and forward motion provides along-track resolution; temporal heterodyne sensing over large temporal bandwidths is required for fine range resolution. Digital holography, also known as spatial heterodyne, can achieve fine resolution in angle-angle space by a combination of a string of apertures in the cross-track direction combined with aperture synthesis in the along-track direction; it can employ narrow laser bandwidths but must still interfere the return field from the object with a local oscillator, requiring stable local oscillator distribution from a master laser to all the telescopes. One could employ multiple small apertures on a moving ground vehicle, underneath the wings of an aircraft, or on a group of small satellites, to synthesize a large 2-D aperture with fine resolution. All of the images from laser illumination systems exhibit speckle in the images that degrade the effective resolution unless one gathers multiple speckled images, with different speckle realizations, and averages together their intensities.

Because of a desire to avoid the complications of local oscillators, including distribution, stability, relative Doppler, and timing, this paper considers an alternative imaging architecture similar to digital holography but employing direct detection and phase retrieval instead of spatial heterodyne. The technique requires, for each telescope, the simultaneous detection of the received beam in at least two planes, where typically one would select an image plane, where one obtains a low-resolution intensity image of the object, and a pupil plane (which is a re-imaged aperture plane). Then one would use a phase retrieval algorithm to reconstruct the field in the plane of the aperture. This is done for each laser pulse and for each telescope within an array of telescopes. An example of a system configuration is shown in Section 2 of this paper. Now having the fields within each aperture position, one can synthesize a larger coherent aperture. Since the relative phases between the different apertures will be unknown, these relative phases must be reconstructed from the measured and processed data. Uncertainties in the relative pointing of the different telescopes results in relative linear phase errors and uncertainties in the relative distances from the object center and each telescope results in piston errors between telescopes, and these are assumed to change for different laser pulses and for different telescopes. These phase errors must be sensed and corrected from the measured and processed data. Section 3 of this paper describes the algorithms developed for these purposes and shows that successful image reconstruction and inter-aperture phasing can (in simulation) be accomplished even for very low signal-to-noise ratios (SNRs), as low as 4 photons per speckle within the detection planes, equivalent a SNR of 2. It also shows the effect on image quality of having different numbers of speckle realizations, each of which requires an additional synthetic aperture of data to be

collected. It is recommended that on the order of ten speckle realizations of each image be collected for high-contrast objects and possibly more for low-contrast objects.

Section 4 of this paper examines system requirements, including pulse repetition frequency and laser coherence length, and derives the relationship between laser power, wavelength, area of the scene illuminated, and other parameters. The area coverage rate, collecting multiple images, is shown to be proportional to the laser power available and inversely proportional to the number of speckle realizations averaged to get one image.

2. SYSTEM ARCHITECTURE

For the purpose of performing systems analysis and simulations, a particular reference approach was chosen. Many variations on this theme are possible. The top of Figure 1 shows an example of a sparse array of apertures, one small aperture (i.e. pupil) per small telescope, moving together. Employing several short laser pulses, they advance downward in the vertical direction and synthesize the larger aperture shown at the bottom. The aperture transmitting the laser illumination beam can be one of the receive apertures or can be another telescope which is either moving along with the receive array (approximately monostatic case, which we will assume here) or can be somewhere entirely different (bistatic case). Furthermore, the single transmitter can be replaced with multiple spatially separated transmitters, which can be advantageous from the point of view of rapidly synthesizing a large aperture from a smaller number of telescopes. There are many possibilities for the number and arrangement of transmitters and receivers to achieve a desired synthetic aperture.

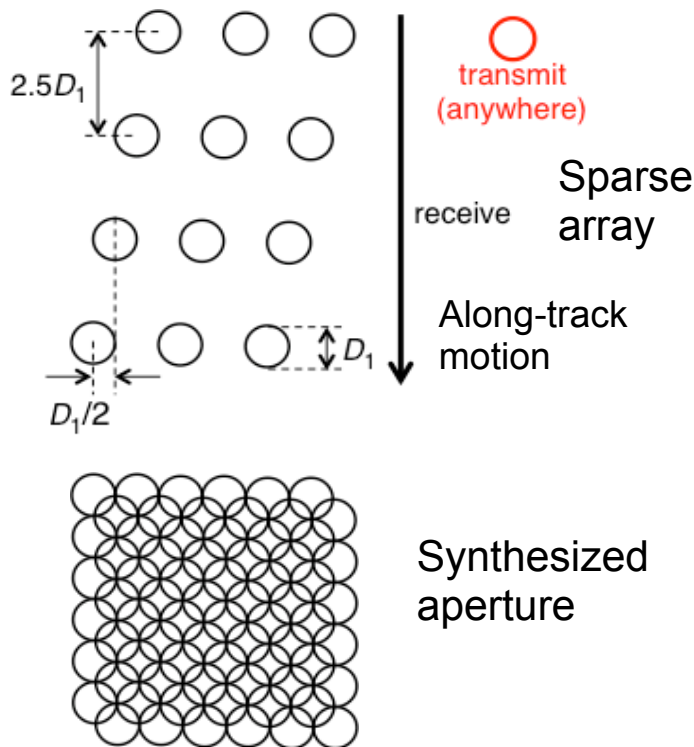


Figure 1. Face-on view of array of telescopes. Top: Sparse array of telescope apertures moving together; D_1 is the diameter of one of the telescope apertures. Bottom: roughly square aperture synthesized from telescope pupils using multiple laser pulses (some of the synthesized aperture outside the square area are not shown).

Aperture synthesis with coherent electromagnetic radiation (laser light) requires that the optical fields be sensed. This is commonly done by heterodyne techniques, interfering the receive field with a local oscillator (LO) or, in holographic terms, a reference beam. Due to an assortment of difficulties in dealing with the LO for an array of receivers, we wish to obtain complex-valued fields from direct detection of intensity. This can be accomplished with a collection approach shown in Figure 2 [1].

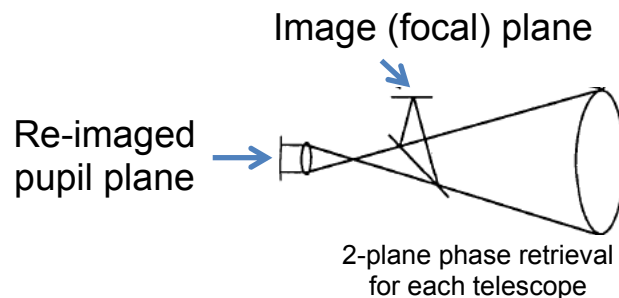


Figure 2. Side view of single telescope, with the object to the right, using 2-plane detection to determine the optical fields with phase retrieval (a subset of a system shown in [1]).

If one collects a 2-D array of speckle intensity in each of two planes, then one can recover a diffraction-limited field across the entrance aperture (the large lens on the right) using a phase-retrieval algorithm [2,3]. Each of the telescopes shown in the top of Figure 1 would employ a pair of detection planes. The detection planes would most likely be in the pupil plane of the telescope and in an image plane, as illustrated here, but other planes (and numbers of planes) are possible as well.

The fields within each of those pupils would have a random piston phase relative to one another. They would also likely have a random tip/tilt phase as well, corresponding to a translation of the image (due to non-identical pointing of the different telescopes) relative to all the other pupils. The exact locations where the reconstructed pupil fields should be located within the synthetic aperture might also be known with insufficient accuracy if the locations of the telescopes with respect to one another are imperfectly known. Solving for these unknown phase and location terms would presumably be possible since they represent at most, 5 additional parameters per aperture, as compared with thousands of phase values being solved by the phase retrieval algorithm. The overlap of the different neighboring apertures making up the synthetic aperture, seen in Figure 1, is very important for making the estimation of these 5 additional parameters robust. Note that if one were to use annular apertures, as shown in Figure 3, then one still retains the overlap regions essential for solving for those additional parameters. While annular apertures do not perform quite as well as filled apertures (since some of the field is missing), we will show later that high-quality images can be reconstructed with annular apertures.

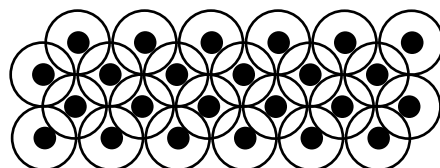


Figure 3. Portion of synthetic aperture for annular-aperture telescopes.

It is also physically possible to reconstruct fields from a single intensity measurement [4], but that approach places stringent demands on the illumination beam and lacks the high degree of robustness that we seek. For the sake of a more robust phase retrieval algorithm, we will consider a two-plane direct detection approach for which each aperture has two planes of intensity measurements, and no LO.

An alternative to the architecture described above is Fourier ptychography [5,6]. It is a method for synthesizing a coherent aperture from image-plane intensities, mostly used for microscopy. In the remainder of this paper we will analyze only the two-plane phase retrieval approach, but the Fourier ptychography approach (also employing phase retrieval), while very different in some respects, is expected to have performance that is in the same ballpark as two-plane phase retrieval.

3. IMAGE RECONSTRUCTION ALGORITHMS AND SIMULATION EXPERIMENTS

As mentioned earlier, the first step is to use a Gerchberg-Saxton type of iterative algorithm to reconstruct the complex-valued field within each aperture. Step 2 is to assemble the reconstructed fields into a synthetic aperture; while doing so, it is necessary to correct piston tip and tilt terms from the different telescopes. This was done using a fast sub-pixel registration algorithm [7], employing the overlap regions of the neighboring apertures within the synthetic aperture. For the simulations reported here, it was assumed that the transverse translations of the telescopes was known; hence we are

solving for 3 additional unknowns per telescope.

Past experience shows that it is the number of photons per speckle that counts for image quality. For digital experiments, if the object field fills the array of numbers, then there is one speckle per sample in the aperture field obtained by computing a fast Fourier transform (FFT) of the object array. If the object fills a width of $1/(q_{ap})$ times the width of the array, then the aperture field will have one speckle per q_{ap} pixels in each dimension, where q_{ap} is the sampling ratio in the aperture, relative to Nyquist sampling. $q_{ap} = 1$ is Nyquist sampled for the fields and $q_{ap} = 2$ is Nyquist sampled for the intensities. For our experiments we added only shot (photon) noise to the measurements, that being the most fundamental source of noise. Further realism would be had by adding detector read noise, dark current, background noise, quantization noise, etc.

3.1 6-aperture Simulations

A large number of data sets were simulated and images were reconstructed, with the 6-aperture synthetic aperture shown in Figure 4 for the purpose of speed. When showing these synthetic apertures here, the sums of the circular apertures are shown, but the actual synthetic aperture is averaged in the areas of overlap rather than summed. For reference, an ideal incoherent image through a single one of the six apertures is shown in Figure 5. In this rendition of the 1954 US Air Force bar target, the finest pair of three bars that can easily be distinguished is indicated by the arrow, which is group 1, element 6, or (1,6) for short.

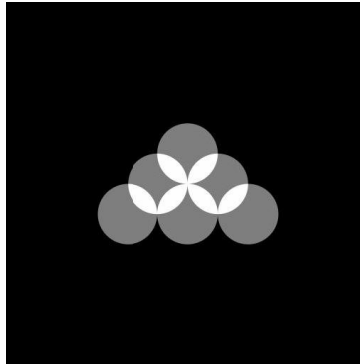


Figure 4. 6-aperture synthetic aperture

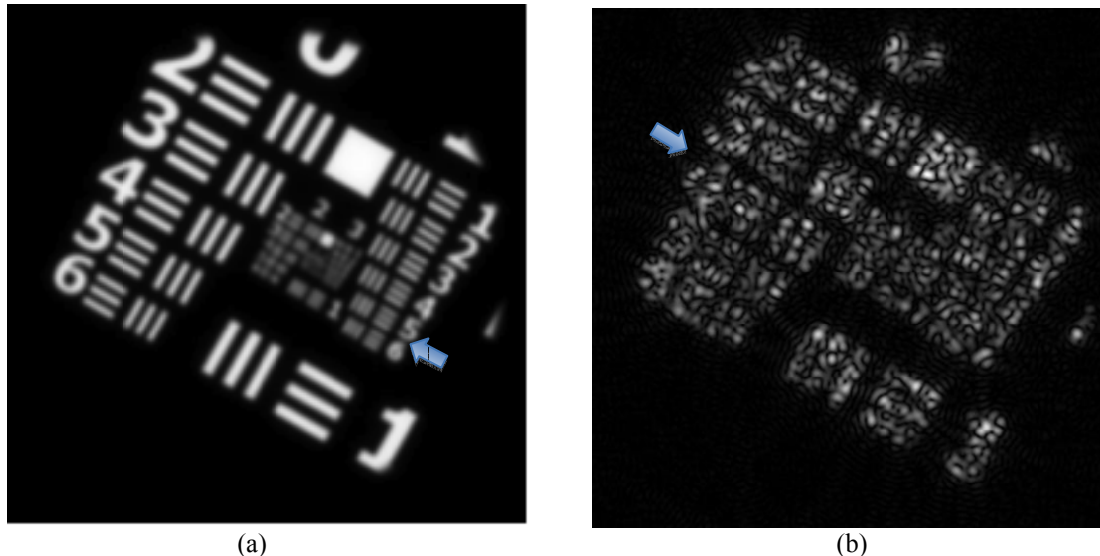


Figure 5. (a) Ideal incoherent image through a single aperture; (b) Ideal coherent, speckled image through a single aperture

Each group is worth a factor of two in resolution, or $\Delta\text{NIIRS} = 1$, where NIIRS is the National Image Interpretability Rating Scale [8], and each element is worth a factor of $2^{1/6} = 1.12246$, or 12.2% additional resolution. Each ΔNIIRS of 0.1 is worth a resolution

factor of $2^{0.1} = 1.0718$. Or, equivalently, each additional group is worth 1 NIIRS and each additional element is worth $1/6 = 0.167$ NIIRS. In the image analyst community, a delta-NIIRS of 0.1 is considered to be just discernible. Hence a delta-element, being worth 0.167 delta-NIIRS, would be significantly greater (1.67 times) than just discernible. Table 1 shows the relationship between delta-groups, delta-elements, delta-NIIRS and ratios of effective resolution.

Table 1. Relationship between delta-groups, delta elements, delta-NIIRS and resolution ratio.

<u>delta groups</u>	<u>delta elements</u>	<u>delta NIIRS</u>	<u>resolution ratio</u>
0	0	0	1
0	0.5	0.083	1.059
0	1	0.167	1.122
0	2	0.333	1.260
0	3	0.500	1.414
0	4	0.667	1.587
0	5	0.833	1.782
<u>0</u>	<u>6</u>	<u>1.000</u>	<u>2.000</u>
1	0	1.000	2.000
1	1	1.167	2.245
1	2	1.333	2.520
1	3	1.500	2.828
1	4	1.667	3.175
1	5	1.833	3.564
<u>1</u>	<u>6</u>	<u>2.000</u>	<u>4.000</u>
2	0	2.000	4.000
2	1	2.167	4.490
2	2	2.333	5.040
2	3	2.500	5.657
2	4	2.667	6.350
2	5	2.833	7.127
<u>2</u>	<u>6</u>	<u>3.000</u>	<u>8.000</u>
3	0	3.000	8.000

For comparison with the incoherent image, in which we can discern (1,6), Figure 5(b) shows an ideal coherent, speckled image through the same single aperture, in which we can discern (0,3) or (0,4), or 1 group plus 2 or 3 elements worse resolution, equivalent (according to Table 1) to a loss of 1.3 to 1.5 in NIIRS and a factor of 2.5 to 2.8 in resolution. When viewing such poor images, one should “zoom out” or demagnify the image, to put the finest detail within a favorable part of the contrast sensitivity curve of the human visual system in order to discern the greatest detail. Note that for much larger synthetic apertures, as will be shown later, one must zoom in or magnify the images to see the finest detail.

From these results we see that the effect of speckle in coherent imaging (of any type) of rough objects plays a major role in effective resolution (a factor of 2.5 to 3) and image interpretability. Speckle is much more dominant for optical and near-infrared than it is for microwave synthetic aperture radar (SAR), at which wavelength the world is much smoother and objects often contain multiple glints that can aid in target recognition.

By gathering multiple (N_s) images with different transmitter/receiver locations relative to the object, each image having a different realization of the speckle pattern, one can average the speckled intensities together to yield a reduced-speckle image that approaches an incoherent image as the N_s approaches infinity. The speckle contrast, initially unity, is reduced by the factor $1/\sqrt{N_s}$ [9]. Figure 6 shows an ideal speckle-reduced image with $N_s = 100$ from a single aperture. It has a noisier appearance than the ideal incoherent image shown above, but it has almost the same resolution. Figure 7(a) shows an ideal speckle-reduced image with $N_s = 100$ from the 6-aperture synthetic aperture. With (2,6) discernible, it has a full factor of two better resolution than the single-aperture image, on account of the synthetic aperture having approximately twice the effective width as the single aperture.

Simulating data with $N_{pps} = 4$ photons per speckle, performing the image reconstruction (including 2-plane phase retrieval and correcting PTT phase for each aperture) with $N_s = 100$ gave the image shown in Figure 7(b). (PTT stands for the relative piston, tips, and tilt phases for each aperture.) Its resolution and quality is only slightly degraded relative to that of the ideal (noise-free) image shown in Figure 7(a), demonstrating that our 2-plane pupil field reconstruction algorithm and aperture phasing algorithm are working well, and that the low light level $N_{pps} = 4$ allows a reasonable reconstruction for this high-contrast object.



Figure 6. Ideal single-aperture speckle reduced image, the average of $N_s = 100$ image intensities.

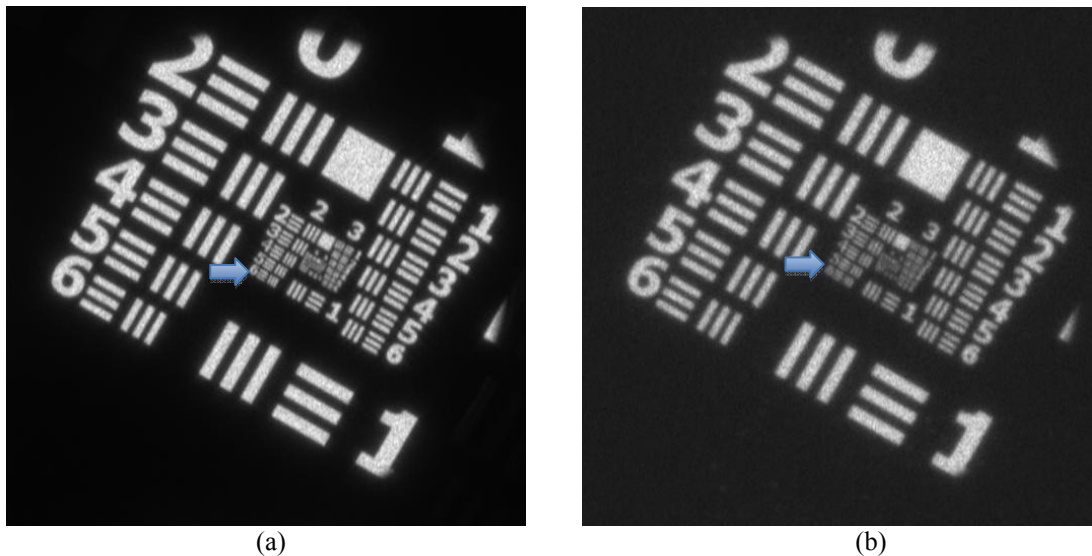


Figure 7. (a) Ideal image from 6-aperture synthetic aperture; (b) Reconstructed image for 6-aperture synthesis with $N_{pps} = 4$, $N_s = 100$.

Table 2 shows results from a number of reconstructions for a variety of signal levels and speckle realizations averaged for this high-contrast object. It shows the importance of having at least several speckle frames over which to average. Averaging over 10 speckle frames improved the resolution by a factor of 2. It also shows that resolution does not improve much above $N_{pps} = 2$ or 4 (very low light levels), for this high-contrast object; the reconstruction algorithms worked very well even for these very low signal levels.

Table 2. Results of image reconstruction for 6-aperture synthesis for varying number of photons per speckle (N_{pps}) and number of speckle realizations averaged (N_s). Top line: group, element just discernible; bottom line: delta-NIIRS relative to ideal incoherent image.

		N_s		
N_{pps}	Infinity	100	10	1
Infinity w/o reconstruct	3,1 0	2,6 - 3,1 0.083	2,4 - 2,5 0.416	1,5 1.333
100		2,6 - 3,1 0.083	2,4 - 2,5 0.416	1,5 1.333
4		2,5 - 2,6 0.250	2,2 - 2,3 0.583	1,3 - 1,4 1.583
2		2,4 - 2,5 0.416	2,1 - 2,2 0.916	1,3 - 1,4 1.583
1		2,2 - 2,3 0.750	1,3 1.667	no bars > 3
0.5		1,1 2.000	no bars > 3	no bars > 3

Group, EI
delta-NIIRS

3.2 72-aperture Simulations

Figure 8(a) shows a 72-aperture synthetic aperture on which further simulation and reconstruction experiments were performed. Note that its individual apertures are somewhat smaller than the ones used for the 6-aperture synthetic aperture above. Figure 8(b)-8(d) show reconstructed images with this larger aperture for $N_{pps} = 100$ and $N_s = 100, 10,$ and $1,$ respectively. With $N_s = 100,$ the image is comparable to the ideal, noise-free image (not shown). With $N_s = 10,$ the image has a noisier appearance, but the resolution is degraded only by approximately a single element. With $N_s = 1,$ the image is much noisier looking (speckle noise), and its resolution is degraded by a factor of two. These results show that the image reconstruction algorithm also works for large synthetic apertures with good SNR = 10. When the SNR was reduced to 2 ($N_{pps} = 4$), however, the aperture phasing algorithm did not work as well, and the image resolution suffered substantially. The phasing algorithm started with a central aperture and boot-strapped its way out to the edges. In the future, the reconstruction could be fixed in two ways. First, one could use a least-squares phasing algorithm, analogous to the kind used to reconstruct phases for a Shack-Hartmann wavefront sensor, but using the cross-correlations of image fields and using both piston and tip-tilt phases. Second, with that as an initial estimate, one could perform another algorithm, such as an image sharpening algorithm [10], to re-estimate the array phasing parameters.

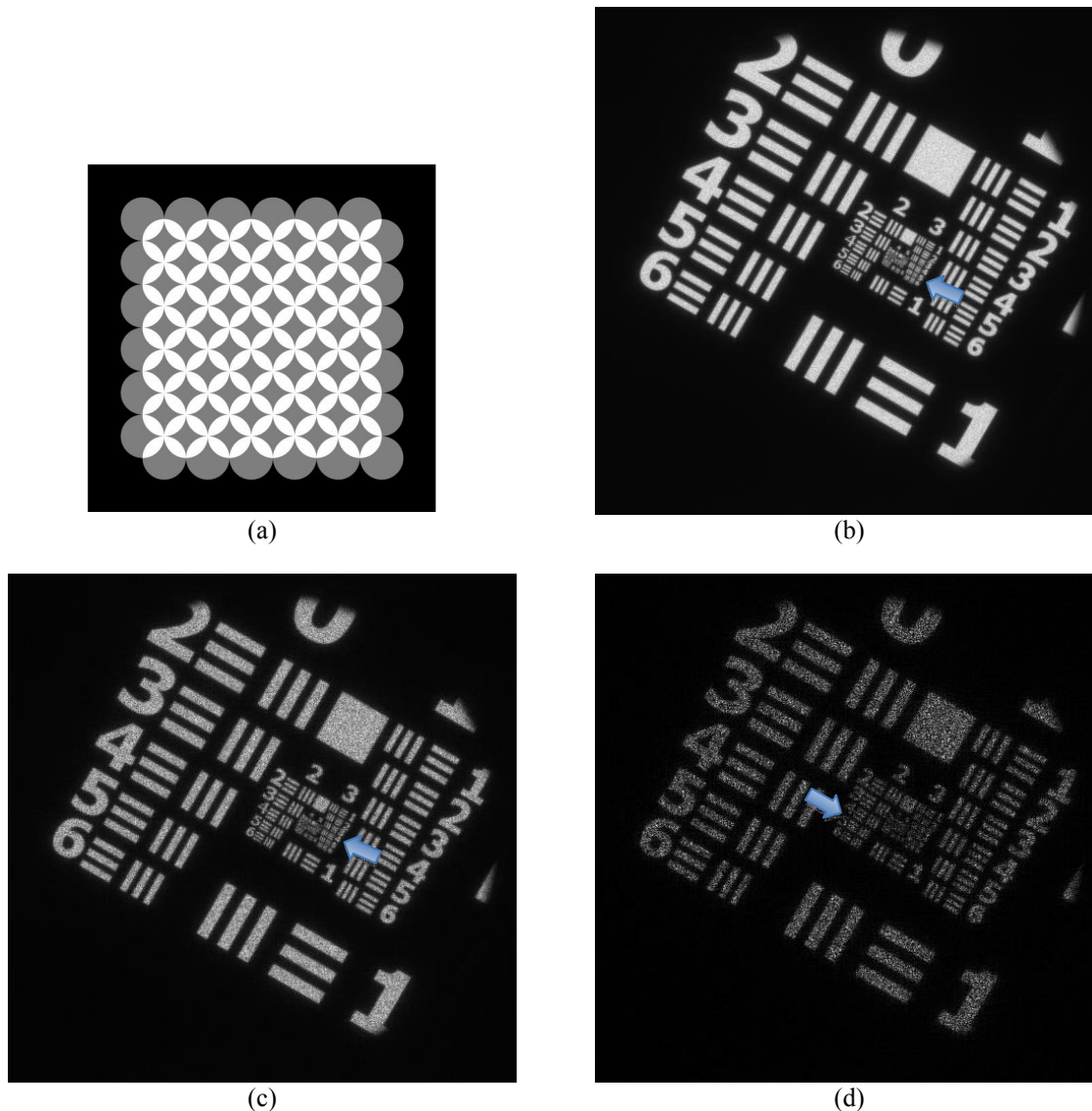


Figure 8. (a) 72-aperture synthetic aperture; Reconstructed images for 72-aperture synthesis with (b) $N_{pps} = 100$, $N_s = 100$; (c) $N_{pps} = 100$, $N_s = 10$; (d) $N_{pps} = 100$, $N_s = 1$.

3.3 72-annular-aperture Simulations

Experiments were performed on annular apertures, which could present a problem if they were configured such that parts of the synthetic aperture were missing. The synthetic-aperture and the corresponding point-spread function used to explore this issue are shown in Figure 9. Cassegrain telescopes having central obscurations that were 33% the diameter of the aperture were assumed. The same aperture synthesis geometry as for the previous filled apertures was used. Significant areas of the synthesized aperture were missing. Note that the actual synthesized aperture would be unity wherever the array shown is greater than zero.

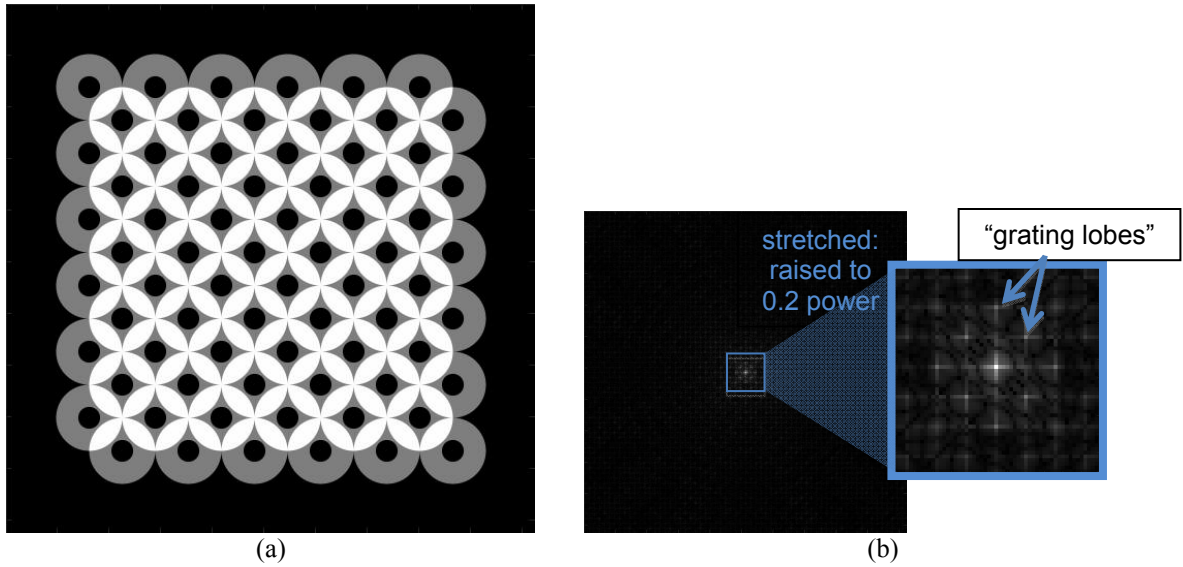


Figure 9. (a) 72-annular-aperture synthetic aperture, (b) point-spread function (stretched in contrast) due to annular synthetic aperture. It contains the “grating lobes” due to the periodicity of the synthetic aperture; they are essentially weaker versions of the central PSF in a halo around it.

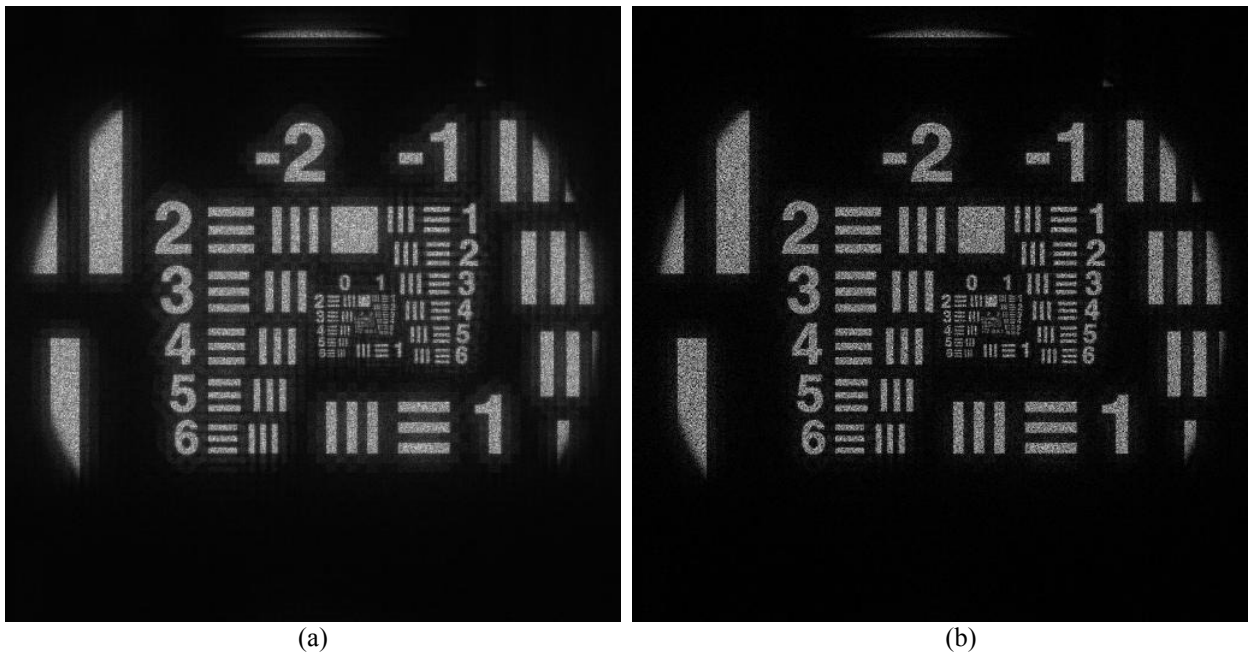


Figure 10. Images from 72-annular aperture synthesis, for $N_s = 10$. (a) Ideal (noise-free) image, showing faint halos; Wiener-Helstrom filtered version of the ideal (noise-free).

Figure 10(a) shows the ideal, noise-free image, with $N_s = 10$, of another USAF bar target rotate to have its edges along the cardinal axes, with the supposition that the effect of the grating lobes would be most severe in that rotation. One can see faint halos around all of the bright parts of the image (they might not show up well in the reproduction here). Figure 10(b) shows the effect of applying a Wiener-Helstrom filter [11] to that image; it greatly reduces the energy in the halos, demonstrating that this filter, meant for incoherent images, does work well for as few as 10 speckle realizations. Reconstruction simulations varying the SNR found that for annular apertures the phasing algorithm did not work well

enough for $N_{pps} = 4$ but did work well for higher SNRs for large (72-aperture) synthetic apertures. For smaller synthetic apertures (e.g. 9 apertures), the phasing algorithms worked well for low SNRs. From this result we can see that, while performance is undoubtedly somewhat worse for annular apertures (they collect fewer photons and they cause unfavorable non-ideal PSFs which, when corrected by the filter, will still cause an increase in noise in the image), we can still successfully use annular apertures for this imaging approach.

3.4 Aperture Array Phasing Accuracy

The relative phasing of the different apertures within the synthetic aperture, including relative piston, tips, and tilt (PTT) phases where the TT phases are equivalent to telescope relative pointing errors, were corrected with a sub-pixel accuracy registration algorithm. The requirements on the accuracy can be thought of as follows. For images, if one has an rms pointing error of s diffraction-limited resolution elements, then the net resolution element width (here, the final resolution of the synthesized aperture) will be approximately $\sqrt{1 + s^2}$ diffraction-limited resolution elements. In that case, a misregistration by 0.25 resolution elements rms will degrade the resolution by a factor of 1.03, a misregistration by 0.5 resolution elements rms will degrade the resolution by a factor of 1.12 (one element in the bar target), and a misregistration by 1 resolution element rms will degrade the resolution by a factor of 1.41 (three elements in the bar target). Based on those numbers, one might require a residual telescope pointing error, after correction, to be around 0.5 resolution elements or less.

In the 72-aperture simulations done earlier for the high-contrast bar targets for $N_{pps} = 100$, the actual pointing errors in the estimates from the noisy data were 0.12 resolution elements rms, which are negligible. For $N_{pps} = 4$ the actual pointing errors in the estimates from the noisy data were 0.77 resolution elements rms, somewhat greater than the goal of 0.5 resolution elements, yielding a non-negligible error. This error would probably be lower than 0.5 if the data were fed into a least-squares reconstruction algorithm, which we did not have a chance to do. This becomes a bigger problem with a realistic-contrast scene than with the high-contrast bar targets, but the size of the effect has not yet been quantified. For a realistic-contrast target it appeared that for $N_{pps} = 4$ the phasing algorithm was yielding significant residual errors whereas for $N_{pps} = 100$ the phasing algorithm was working very well.

4. PRACTICAL CONSIDERATIONS

Several practical issues must be addressed to make feasible this multi-aperture direct-detection synthetic-aperture, active, coherent imaging system concept. The system architecture shown in Figure 1 was assumed, although the analysis could be readily applied to other cases.

The pulse repetition frequency (PRF) of the laser must be sufficient to allow no gaps in the synthetic aperture. The PRF must be fast enough so that, for the example of four rows of apertures shown in the top of Figure 1, the first row of telescopes moves forward by half its diameter between pulses (the speckles move across the aperture at twice the speed that the aperture moves forward, since both the apertures and the transmitter are moving forward at the same speed). From the bottom of that figure, the first telescope pupil in the synthetic aperture appears again one diameter from its previous position. This is the general rule for monostatic synthetic-aperture radar. A fast PRF, however, requires detector arrays that are equally fast; an array of avalanche photo-diodes (APDs), for example, could easily keep up. As mentioned in the image reconstruction section, in order to achieve adequate image quality, multiple synthetic-aperture images, each with an independent speckle pattern, are usually desired. Collecting multiple speckle patterns seems to be less expensive than building a much larger synthetic aperture to achieve the desired resolution. The length of an individual pulse should be short enough to freeze the speckles at the detector, or one must have an optical compensation for translating speckles. The speckles will be moving at twice the speed of the imaging platform, assuming that the laser illuminator is near the receiver traveling at approximately the same velocity. The diameter of one of the speckles in the pupil plane will be

$$d_s = \frac{\lambda R}{w_o} \quad (1)$$

where w_o is the width of the illuminated area of the ground (projected onto the line of sight). One would like to have two samples per speckle. Since the pupil-plane detection is designed to be performed on a demagnified image of the pupil, as shown in Figure 2, the sample spacing of the detector array will be reduced by the magnification factor, but the number of samples remains the same. If the speckles are moving too quickly across the aperture during a pulse, it may be necessary to have, as part of the receiver, optics that scans along with the speckle motion to freeze it over a longer pulse

length. The individual pulses should have a coherence length that is at least twice the depth of the illuminated object in order for the entire field from the object to interfere.

If the product of the two-way atmospheric transmittance, transmitter and receiver optical transmittance and quantum efficiency is η , and the mean object intensity reflectivity is τ_o , then a laser pulse with energy E_p joules (per pulse) at range R , reflected from the object area and falling onto a single collecting element of length and width d_d results in a mean number of photons at a pupil-plane detector of

$$N_{pd} = E_p \tau_o \eta \lambda d_d^2 / (2\pi R^2 hc), \quad (2)$$

where h is Planck's constant, c is the speed of light, and a Lambertian reflecting surface is assumed. A factor of 2 in the denominator comes from the fact that half of the light goes to a pupil-plane detector array and the other half goes to an image-plane detector array. For simplicity we assume the detector pitch is also d_d (unity duty cycle). Since it is photons per speckle that determines image quality, employing Eq. (1) we have the number of photons per speckle is

$$N_{pps} = \frac{E_p \tau_o \eta \lambda d_s^2}{2\pi R^2 hc} = \frac{E_p \tau_o \eta \lambda^3}{2\pi hc w_o^2}. \quad (3)$$

For a given wavelength and pulse energy, we see that there is a direct trade-off between the number of photons per speckle and the area, w_o^2 , of the illuminated object or scene. Solving for the illuminated width that gives a desired N_{pps} (~ 4 for a high-contrast object, according to our image reconstruction simulations) we get

$$w_o = \sqrt{\frac{E_p \tau_o \eta \lambda^3}{2\pi hc N_{pps}}}. \quad (4)$$

It is interesting to note that this expression is independent of range and independent of resolution! For a given resolution, if one doubles the range, then the aperture must double in diameter, which results in gathering the same total number of photons. For a given range, if one doubles the resolution, then one must double the aperture diameter, gathering four times the number of photons, but those photons are spread over four times as many resolution elements, so the number of collected photons per resolution element (per speckle) stays the same.

Suppose that one has a laser with average power $E_L = 200$ W and that we need $N_{pps} = 4$ photons/speckle (adequate for a high-contrast object), and that $\tau_o = 0.2$ and $\eta = 0.5$ and $\lambda = 1 \mu\text{m}$. Then the equation above predicts the following scenarios.

Case 1. If we have a continuous PRF of 300 Hz (appropriate for a ground-moving vehicle platform), which would give us 0.67 J/pulse, then $w_o = 290$ m. On the other hand, if we had a continuous PRF of 78 kHz (appropriate for a low earth-orbit satellite platform, which would give us 2.6 mJ/pulse, then $w_o = 18$ m, a very tiny instantaneous field of view. However, one could collect many small images and mosaic them together into a larger image.

Case 2. If during one second only 10 laser pulses are transmitted, allowing for a single synthetic aperture, which would allow for 20 J/pulse, then $w_o = 1,590$ m (over 2 square km), but would result in a speckled image.

Case 3. If during one second the laser transmits 70 pulses making up 10 synthetic apertures ($N_s = 10$), for a reduced-speckle image, which would allow for 2.9 J/pulse, then $w_o = 600$ m, collecting about 1/3 square km per second.

Case 3 above is probably closest to the scenarios one would choose to collect, to take advantage of the 10 speckle realizations that gives one the desired image quality.

The above calculations are for the case of a high-contrast object like the USAF bar targets. For objects of more realistic contrast, we have established that larger SNRs (larger values of N_{pps}) and larger numbers of speckle realizations, N_s , are needed, but further simulations would be required to determine how much greater SNRs are needed for lower-contrast objects.

4.1 Fourier Ptychography versus 2-Plane Phase Retrieval

Another direct detection alternative to the architecture analyzed in this paper is Fourier ptychography [12,13]. It is a method for synthesizing a coherent aperture from image-plane intensities, mostly used for microscopy. It involves coherently illuminating the sample from multiple different angles to synthesize a larger aperture. For the applications of interest here, however, similar ideas and algorithms can be used to perform aperture synthesis with moving apertures. It is similar to the aperture synthesis described for the two-plane intensities above, but with the following differences. First, only measurements of the low-resolution focal-plane images are employed. Second, the overlaps of the individual aperture locations within the synthetic aperture are much denser than the overlaps shown in Figure 1. Hence there is much more redundancy within the synthetic aperture and the synthetic aperture will be smaller than, and the resolution will be poorer than, for the two-plane approach for a given number of telescopes and laser pulses. In microscopic imaging applications, Fourier ptychography has been shown to be robust with the dense sampling. Requiring only a single detector array in each telescope rather than a beamsplitter and two detector arrays makes the individual telescopes simpler than the two-plane approach. The image reconstruction is different, too. Rather than reconstructing a field across each pupil, synthesizing an aperture from those fields, and then phasing the pupils within the aperture, in Fourier ptychography the phase retrieval is performed directly on the synthesized array. A single synthesized complex array is found that is consistent with all of the measured low-resolution image intensities. Each measured low-resolution image intensity must agree with the images obtained by computing the Fourier transforms of a circularly (or whatever the shape of the individual telescopes) windowed portion of the estimated synthetic-aperture field (and taking the squared magnitude). Note that no measurements are made in the pupil plane in that case. I would expect the Fourier ptychography approach (also employing phase retrieval) to have performance that is in the same ballpark as two-plane phase retrieval.

5. CONCLUSIONS

From the image reconstruction studies described in Section 2, we learned the following about the 2-plane direct-detection phase retrieval approach to sparse-aperture synthetic-aperture imaging:

- Three sets of algorithms are needed: (1) reconstructing the phase of each pupil from the pupil and image plane intensities, (2) assembly of the pupils into a synthetic aperture and correcting relative phase errors (piston, tip and tilt) based on overlapping portions of the synthesized aperture (the tip and tilt correction corresponding to correcting the relative pointing errors between the telescopes), and possibly (3) pupil registration correction (not discussed here).
- The results of Section 3 show that algorithm (1), individual pupil field reconstruction, worked well even for low SNRs (SNR = 2, equivalent to 4 photons per speckle in each plane of detection).
- Algorithm (2), aperture phasing, worked well for the same low SNRs with modest sized (9 apertures) synthetic apertures, but greater SNRs were needed for large (72-aperture) synthetic apertures. To work well for low SNRs and large synthetic apertures, a least-squares reconstruction algorithm is needed, but time did not permit its implementation.
- More work needs to be done on Algorithm (3), pupil registration, when needed, and such algorithms exist in the literature on template matching employing weighting functions are known.
- Annular-aperture telescopes as well as filled-aperture telescopes can be made to work, despite missing areas within the synthetic aperture. Wiener-Helstrom filtering was effecting in cleaning up halos in the reconstructed images from a speckle-averaged image from annular-aperture telescopes.
- For high-contrast objects, we recommend a minimum of about 4 photons per speckle for high-contrast objects. The requirements for low-contrast objects are for a greater light level, but were not quantified.
- For high-contrast objects, averaging 10 speckle realizations yields about a factor of 2 improvement in resolution (+1 NIIRS) over a single speckle realization. For low-contrast objects a greater number of speckle realizations is needed, but that was not quantified.
- The area coverage rate is proportional to the laser power, the transmittances of the atmosphere and optics, the reflectivity of the object, the quantum efficiency of the detectors and the cube of the wavelength; and it is inversely proportional to the number of photons per speckle needed to achieve the desired image quality. One example: assuming a 200 W average power laser, needing 10 speckle realizations, and needing 4 photons per speckle per plane, using 70 pulses at 2.9 J/pulse, one could image one 600 m x 600 m area or $1/3 \text{ km}^2$ per second.
- The pulse repetition frequency needed to avoid gaps in the synthetic aperture are proportional to the speed of the platform and require fast detector arrays.
- There are many different geometrical configurations of telescope apertures and laser transmitters than can be employed for differing numbers of each, allowing for a flexible imaging architecture.

6. ACRONYMS AND MOST COMMON SYMBOLS

Acronym	Description
APD	avalanche photo-diodes
FFT	fast Fourier transform
LEO	low-earth orbiting
LO	local oscillator
NIIRS	National Image Interpretability Rating Scale
PRF	pulse repetition frequency
PSF	point-spread function
PTT	piston, tip and tilt (phase errors)
SAR	synthetic-aperture radar
SNR	signal-to-noise ratio
N_{pps}	number of photons per speckle
N_s	number of speckle patterns averaged (each another synthetic aperture)

This research was developed with funding from the Defense Advanced Research Projects Agency (DARPA).

The views, opinions and/or findings expressed are those of the author and should not be interpreted as representing the official views or policies of the Department of Defense or the U.S. Government.

REFERENCES

- [1] Fienup, J.R. and Kowalczyk, A.M. "Phase Retrieval for a Complex-Valued Object by Using a Low-Resolution Image," *J. Opt. Soc. Am. A* 7, 450-458 (1990).
- [2] Gerchberg, R.W. and Saxton, W.O. "A Practical Algorithm for the Determination of Phase from Image and Diffraction Plane Pictures," *Optik* 35, 237-246 (1972).
- [3] Fienup, J.R., "Phase Retrieval Algorithms: A Comparison," *Appl. Opt.* 21, 2758-2769 (1982).
- [4] Fienup, J.R., "Lensless coherent imaging by phase retrieval with an illumination pattern constraint," *Opt. Express* 14, 498-508 (2006).
- [5] Zheng, G., Kolner, C. and Yang, C., "Microscopy Refocusing and Dark-field Imaging by using a Simple LED Array," *Opt. Lett.* 36, 3987-3989 (2011).
- [6] Zheng, G., Horstmeyer, R. and Yang, C., "Wide-field, High-resolution Fourier Ptychographic Microscopy," *Nat. Photonics* 7, 739-745 (2013).
- [7] Guizar-Sicairos, M., Thurman, S.T., and Fienup, J.R., "Efficient Subpixel Image Registration Algorithms," *Opt. Lett.* 33, 156-158 (2008).
- [8] Leachtenauer, J.C., Malila, W., Irvine, J., Colburn, L., Salvaggio, N., "General Image-Quality Equation: GIQE," *Appl. Opt.* 36, 8322-8328 (1997).
- [9] Goodman, J.W., *Speckle Phenomena in Optics: Theory and Applications*, (Roberts and Company Publishers, 2007).
- [10] Tippie, A.E., Kumar, A., and Fienup, J.R., "High-resolution Synthetic-Aperture Digital Holography with Digital Phase and Pupil Correction," *Opt. Express* 19, 12027-12038 (2011).
- [11] Helstrom, C.W., "Image Restoration by the Method of Least Squares," *J. Opt. Soc. Am.* 57, 297-303 (1967).
- [12] Zheng, G., Kolner, C., and Yang, C., "Microscopy Refocusing and Dark-field Imaging by using a Simple LED Array," *Opt. Lett.* 36, 3987-3989 (2011).
- [13] Zheng, G., Horstmeyer, R., and Yang, C., "Wide-field, High-resolution Fourier Ptychographic Microscopy," *Nat. Photonics* 7, 739-745 (2013).